


 Cite this: *RSC Adv.*, 2021, 11, 13341

 Received 28th January 2021  
 Accepted 1st April 2021

DOI: 10.1039/d1ra00739d

[rsc.li/rsc-advances](http://rsc.li/rsc-advances)

# A ratiometric fluorescent probe for the detection of $\beta$ -galactosidase and its application†

Yanan Li, Bing Deng, Haitao Chen, \* Shaoxiang Yang \* and Baoguo Sun

Herein, a coumarin fluorescent probe (Probe 1) was developed for the ratiometric detection of  $\beta$ -galactosidase ( $\beta$ -gal) activity. The detection range was 0–0.1 U mL<sup>-1</sup> and 0.2–0.8 U mL<sup>-1</sup>, and the limit of detection (LOD) was 0.0054 U mL<sup>-1</sup>. Moreover, the luminous intensity of Probe 1 increased gradually with increase in  $\beta$ -gal activity. It could be observed under 254 nm UV irradiation by the naked eye. Furthermore, this method only required a small amount of sample (20  $\mu$ L) and a short analytical time (30 min) for the detection of  $\beta$ -gal activity with a low LOD. Probe 1 was successfully used to detect  $\beta$ -gal activity in real fruit samples, and can be applied to the quantitative and qualitative detection of  $\beta$ -gal activity.

## 1. Introduction

$\beta$ -Galactosidase ( $\beta$ -gal, EC 3.2.1.23) is part of the glycoside hydrolase family and has many microbial sources.<sup>1</sup> In addition to its hydrolysis activity,  $\beta$ -gal from some sources also exhibits glycosylation activity. Food-processing applications of  $\beta$ -gal mainly include the following: allowing lactose-intolerant individuals to consume dairy; improving the sweetness of dairy products; preventing dairy products from crystallizing during freezing; the production of galactooligosaccharides; applications in fermented dairy products; whey processing; the analysis of lactose content in dairy products; and promoting the softening and ripening of fruit and vegetables.<sup>2–4</sup>  $\beta$ -gal has also been used for improving the sweetness, digestibility, flavor, and solubility of dairy products.<sup>5</sup>

$\beta$ -Galactosidase is widely found in many kinds of plants. Generally, the content of  $\beta$ -gal increases when plants mature,<sup>6</sup> and the activity of  $\beta$ -gal has a positive correlation with the maturity of fruit, including tomato,<sup>7</sup> papaya,<sup>8</sup> apple,<sup>9</sup> persimmon,<sup>10</sup> kiwi fruit,<sup>11</sup> avocado,<sup>12</sup> pear,<sup>13</sup> peach,<sup>14</sup> and mango.<sup>15</sup> It can degrade cell-wall polysaccharides and release free galactose, which can promote – for example – pepper ripening and ethylene production in tomatoes.<sup>7</sup> However, many enzymes exist in different types of fruit. Therefore, the development of a simple, selective, and rapid detection method for  $\beta$ -gal activity in fruit is important.

To date, many methods have been used for the detection of  $\beta$ -gal activity. These include chemiluminescence,<sup>16</sup> HPLC,<sup>17</sup> colorimetric methods,<sup>18</sup> magnetic resonance,<sup>19</sup> UV

spectrophotometry,<sup>20</sup> positron emission tomography,<sup>21</sup> enzyme-linked immunosorbent assay technology,<sup>22</sup> and electrochemical methods.<sup>23</sup> However, there are certain disadvantages associated with these methods, such as long experimental duration, complex operation conditions, and high experimental costs. Thus, developing a selective, rapid, and simple detection method for  $\beta$ -gal activity is necessary for applications in fruit production. To this end, the development of novel fluorescent probes is very promising,<sup>24–29</sup> and many kinds of  $\beta$ -gal probes have been reported for use in biological imaging,<sup>30–32</sup> including two-photon fluorescence probes,<sup>33,34</sup> ratiometric probes,<sup>35,36</sup> and turn-on probes.<sup>37–39</sup> However, fluorescent probes used in fruit detection are extremely rare in scientific literature.<sup>40,41</sup>

To develop a simple detection method for  $\beta$ -gal activity in fruit, a ratiometric fluorescent probe (Probe 1) with high accuracy and detection precision was developed. This ratiometric fluorescent probe has the characteristics of high accuracy and strong anti-interference. Further, the luminous intensity of the Probe 1 solution increased with increasing  $\beta$ -gal activity under 254 nm UV irradiation. In addition, Probe 1 was successfully applied to the quantitative and qualitative detection of  $\beta$ -gal activity in fruit.

## 2. Materials and methods

### 2.1 General methods

The  $\beta$ -gal, sodium chloride (NaCl), magnesium chloride (MgCl<sub>2</sub>), hydrogen peroxide (H<sub>2</sub>O<sub>2</sub>), ammonium chloride (NH<sub>4</sub>Cl), sodium bromide (NaBr), glutathione (GSH, 98%), glycine (Gly), D-leucine (Leu), potassium iodide (KI), histidine (His), potassium chloride (KCl), L-valine (Val),  $\beta$ -glucuronidase (from *Escherichia coli*), lysozyme (from chicken egg whites), lipase (from porcine pancreas), and  $\alpha$ -galactosidase ( $\alpha$ -gal) were purchased from Bailingwei Co., Ltd, China.

Beijing Key Laboratory of Flavor Chemistry, Beijing Technology and Business University, Beijing 100048, China. E-mail: chenht@th.btbu.edu.cn; yangshaoxiang@th.btbu.edu.cn

† Electronic supplementary information (ESI) available. See DOI: 10.1039/d1ra00739d



## 2.2 Instruments

Fluorescence spectra were obtained using the Rili F-4600 fluorescence spectrometer. NMR spectra were obtained using the Bruker AV 300 MHz NMR machine. HRMS was performed using a Bruker Apex IV FTMS.

## 2.3 Synthesis of Probe 1

7-Hydroxy-4-methylcoumarin (0.18 g, 1.00 mmol),  $\text{Cs}_2\text{CO}_3$  (1.63 g, 5.00 mmol),  $\text{Na}_2\text{SO}_4$  (0.36 g, 2.50 mmol), galactopyranosyl-1-bromide (3068-32-4, 0.31 g, 0.75 mmol), and  $\text{CH}_3\text{CN}$  (30 mL) were added to a flask (Scheme 1) and reacted for 1 h at 25 °C to obtain compound 2 (0.35 g, 91% yield).

Compound 2 (0.23 g, 0.4 mmol) was dissolved in  $\text{CH}_3\text{OH}$  (20 mL). A solution of  $\text{K}_2\text{CO}_3$  (0.13 g, 0.09 mmol) and  $\text{CH}_3\text{OH}$  (80 mL) was added and reacted for 4 h at 25 °C, after which the mixture was adjusted to pH 7 using an aqueous  $\text{H}_2\text{SO}_4$  solution (0.05 M). The precipitate was removed by filtration and recrystallized from ethanol to obtain Probe 1 (0.11 g, 81% yield).

$^1\text{H}$  NMR (300 MHz,  $\text{CDCl}_3$ )  $\delta$  (ppm): 7.70 (d,  $J = 9.4$  Hz, 1H), 7.03 (d,  $J = 7.0$  Hz, 2H), 6.24 (s, 1H), 5.21 (s, 1H), 4.98 (d,  $J = 7.6$  Hz, 1H), 4.87 (s, 1H), 4.66 (s, 1H), 4.52 (s, 1H), 3.72 (s, 1H), 3.66 (d,  $J = 6.1$  Hz, 1H), 3.60 (d,  $J = 8.1$  Hz, 1H), 3.53 (s, 2H), 3.45 (s, 1H), 2.41 (s, 3H).  $^{13}\text{C}$  NMR (75 MHz,  $\text{CDCl}_3$ )  $\delta$  (ppm): 160.23, 160.06, 154.39, 153.28, 126.35, 113.99, 113.40, 111.62, 103.17, 100.64, 75.69, 73.20, 70.09, 68.11, 60.37, 18.08. HRMS (ESI): calcd for  $[\text{M} - \text{H}]^-$  337.092891, found 337.0931.

## 2.4 Preparation of analytes

Probe 1 was dissolved using DMSO.  $\beta$ -gal,  $\beta$ -glucuronidase, lysozyme, lipase, and  $\alpha$ -gal were dissolved in Tris-HCl (pH 7.3, 50 mM) and frozen in a -20 °C refrigerator. The stock solution was diluted using a certain concentration gradient with Tris-HCl (pH 7.3, 50 mM) before each use. NaCl, KCl,  $\text{MgCl}_2$ , KI,  $\text{NH}_4\text{Cl}$ , NaBr,  $\text{H}_2\text{O}_2$ , GSH, Gly, Leu, His, and Val, were dissolved in deionized water.

## 2.5 Preparation of samples

Pears, apples, grapes, strawberries, and kiwis were bought from a local supermarket. Twenty grams of the abovementioned fruit

were centrifuged for 10 min, at 12 000 rpm, after grinding; subsequently, the supernatant was obtained, which was filtered and reserved.

## 2.6 Fluorescence detection assays

The Probe 1 solution (1 mM, 0.02 mL) was added to a cuvette, to which 2 mL of water was added. Then,  $\beta$ -gal was added; after 40 min, the mixture was analyzed using fluorescence spectra (slit width = 5 nm,  $\lambda_{\text{ex}} = 327$  nm, voltage = 500 V, and temperature = 37 °C).

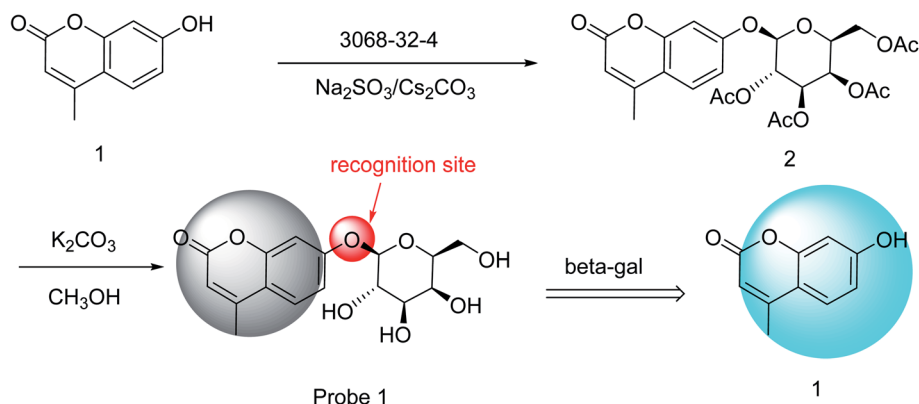
# 3. Results and discussion

## 3.1 Probe preparation

Probe 1 was synthesized in two steps. First, compound 2 was obtained through the nucleophilic substitution of 7-hydroxy-4-methylcoumarin with galactopyranosyl-1-bromide (3068-32-4). Second, the acetyl groups of compound 2 were hydrolyzed to obtain Probe 1 (Scheme 1). Probe 1 was purified by recrystallization from ethanol, and NMR and HRMS were used to characterize this probe (Fig. S1–S3, ESI<sup>†</sup>). The preparation process was carried out at 25 °C under mild conditions; thus, the synthesis of Probe 1 was a simple process.

## 3.2 Fluorescence properties

First, the fluorescence response of Probe 1 with  $\beta$ -gal in different solutions ( $\text{CH}_3\text{CN}$ ,  $\text{H}_2\text{O}$ , DMSO,  $\text{C}_2\text{H}_5\text{OH}$ , and THF) was determined (Fig. 1a). After the addition of  $\beta$ -gal, the fluorescence intensity was decreased at 374 nm in  $\text{CH}_3\text{CN}$ , DMSO,  $\text{C}_2\text{H}_5\text{OH}$ , and THF, with changes in only one fluorescent emission. In  $\text{H}_2\text{O}$ , however, the fluorescence intensity was decreased at 374 nm and significantly increased at 444 nm. As shown in Fig. 1b, Probe 1 displayed a fluorescence emission peak at 374 nm in an  $\text{H}_2\text{O}$  solution. After the addition of  $\beta$ -gal, the fluorescence intensity at 374 nm decreased and a peak appeared at 444 nm. The fluorophore (7-hydroxy-4-methylcoumarin, compound 1) had a peak at 444 nm in an  $\text{H}_2\text{O}$  solution. This confirmed that 374 nm was the peak of Probe 1 and 444 nm was the fluorescence-emission peak of the fluorophore. These results indicated that Probe 1 was



Scheme 1 Synthesis of Probe 1 and the recognition mechanism of Probe 1 to  $\beta$ -gal.



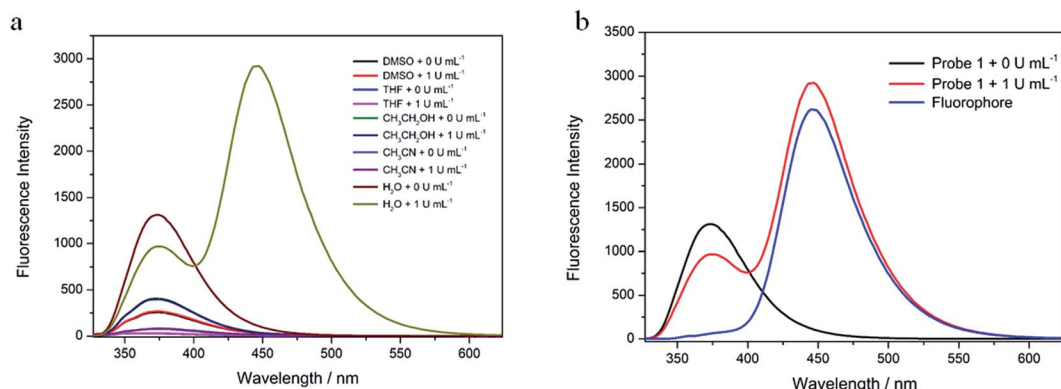


Fig. 1 (a) Fluorescence spectra of Probe 1 (10  $\mu\text{M}$ ) and Probe 1 in the presence of  $\beta\text{-gal}$  (1  $\text{U mL}^{-1}$ ) in  $\text{CH}_3\text{CN}$ ,  $\text{H}_2\text{O}$ ,  $\text{DMSO}$ ,  $\text{C}_2\text{H}_5\text{OH}$  and  $\text{THF}$  at  $37^\circ\text{C}$ . (b) Fluorescence spectra of Probe 1 (10  $\mu\text{M}$ ), compound 1 (10  $\mu\text{M}$ ) and Probe 1 in the presence of  $\beta\text{-gal}$  (1  $\text{U mL}^{-1}$ ) in  $\text{H}_2\text{O}$  at  $37^\circ\text{C}$ .

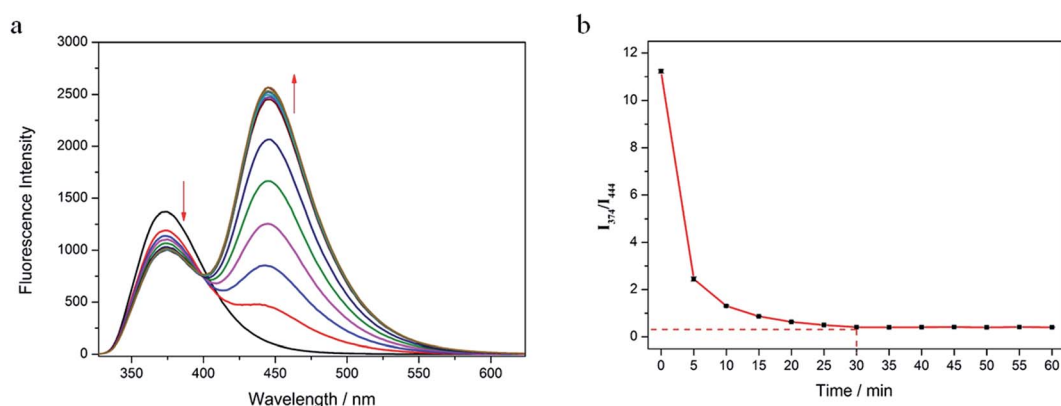


Fig. 2 (a) Time-dependent fluorescence spectra of Probe 1 (10  $\mu\text{M}$ ) in the presence of  $\beta\text{-gal}$  (1  $\text{U mL}^{-1}$ ) in water at  $37^\circ\text{C}$ . (b) The fluorescence emission ratio ( $I_{444\text{ nm}}/I_{374\text{ nm}}$ ) of Probe 1 in the presence of  $\beta\text{-gal}$  from 0 min to 60 min. Tests were performed in triplicate.

a ratiometric probe, facilitating the detection of  $\beta\text{-gal}$  by determining the ratio of fluorescence intensity at two different emission wavelengths.

Second, the time-response relationships of Probe 1 toward  $\beta\text{-gal}$  in water were tested (Fig. 2a). The fluorescence intensity at 374 nm decreased slowly with the addition of  $\beta\text{-gal}$ . Simultaneously, the fluorescence intensity at 444 nm increased rapidly. The fluorescence emission ratio ( $I_{444\text{ nm}}/I_{374\text{ nm}}$ ) decreased rapidly from 0 to 10 min, and reached an equilibrium in 30 min (Fig. 2b). The emission ratio remained unchanged from 30 to 60 min. This shows that 30 min were required for the identification of  $\beta\text{-gal}$  by Probe 1, which was set as the duration for the subsequent experiments.

The effects of competitor ions and compounds were used to ascertain the selectivity of Probe 1. Various competitors were tested, including  $\text{Na}^+$ ,  $\text{K}^+$ ,  $\text{Mg}^{2+}$ ,  $\text{I}^-$ ,  $\text{NH}_4^+$ ,  $\text{Br}^-$ ,  $\text{H}_2\text{O}_2$ ,  $\text{Cl}^-$ , GSH, Gly, Leu, Val, His,  $\beta\text{-glucuronidase}$ , lipase, and lysozyme (Fig. 3). In the presence of any of these competing ions and compounds, there was minimal change in the emission ratio ( $I_{444\text{ nm}}/I_{374\text{ nm}}$ ). In particular, Probe 1 was almost unresponsive in the presence of  $\beta\text{-glucuronidase}$  and  $\alpha\text{-gal}$ . However, with the addition of  $\beta\text{-gal}$ , the emission ratios ( $I_{444\text{ nm}}/I_{374\text{ nm}}$ ) of Probe 1 +  $\beta\text{-gal}$  and Probe 1 +  $\beta\text{-gal}$  + competitors were

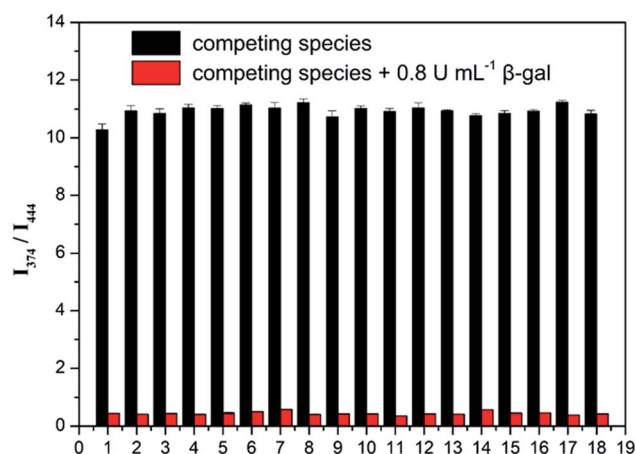


Fig. 3 The fluorescence emission ratio ( $I_{444\text{ nm}}/I_{374\text{ nm}}$ ) of Probe 1 (10  $\mu\text{M}$ ) upon addition of various species (0.8  $\text{U mL}^{-1}$  for  $\alpha\text{-gal}$ , lipase and 100  $\mu\text{M}$  for others). 1, blank; 2,  $\text{Na}^+$ ; 3,  $\text{K}^+$ ; 4,  $\text{Mg}^{2+}$ ; 5,  $\text{I}^-$ ; 6,  $\text{NH}_4^+$ ; 7,  $\text{Br}^-$ ; 8,  $\text{H}_2\text{O}_2$ ; 9, GSH; 10, Gly; 11, Leu; 12, His; 13, Val; 14,  $\beta\text{-glucuronidase}$ ; 15, lysozyme; 16, lipase; 17,  $\alpha\text{-gal}$ ; 18,  $\text{Cl}^-$ . 0.8  $\text{U mL}^{-1}$  for  $\beta\text{-gal}$ . Tests were performed in triplicate.



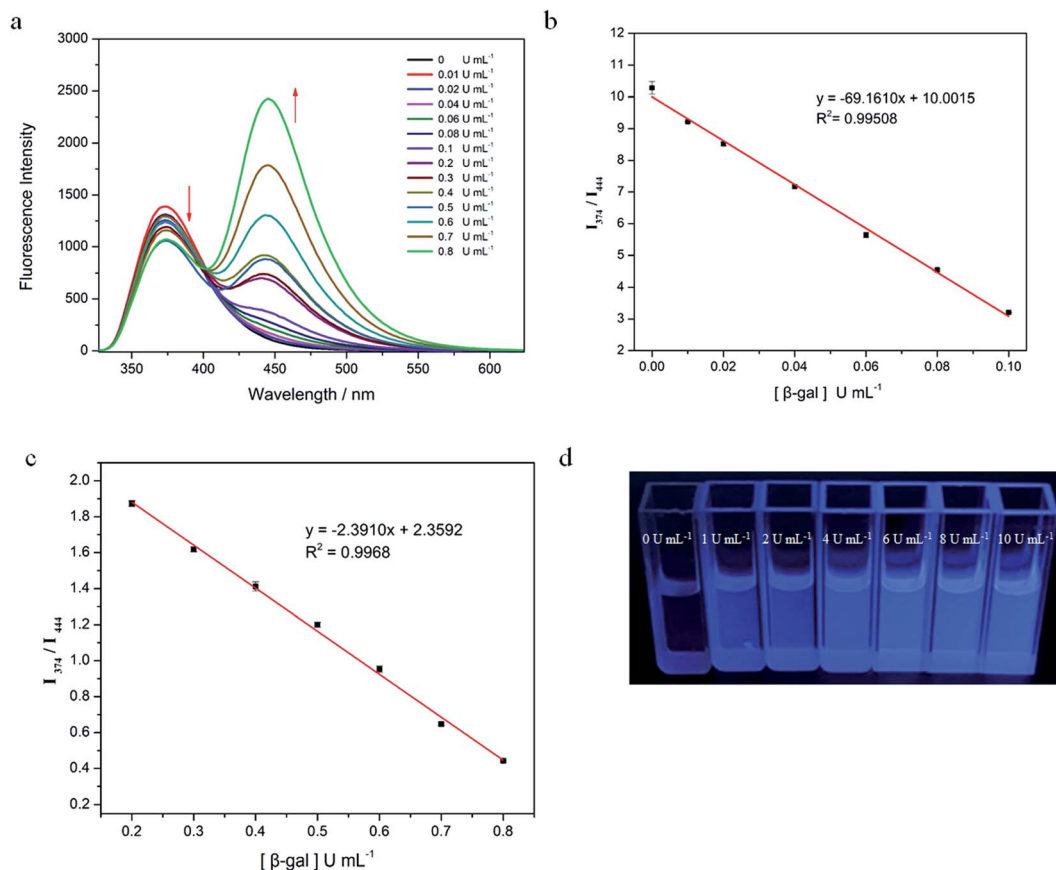


Fig. 4 (a) Fluorescence spectra of Probe 1 (10 μM) with β-gal (0, 0.01, 0.02, 0.04, 0.06, 0.08, 0.1, 0.2, 0.3, 0.4, 0.5, 0.6, 0.7, 0.8 U mL<sup>-1</sup>). (b) Plot of fluorescence intensity differences with 0–0.1 U mL<sup>-1</sup> β-gal. (c) Plot of fluorescence intensity differences with 0.2–0.8 U mL<sup>-1</sup> β-gal. Tests were performed in triplicate. (d) Photograph of Probe 1 (10 μM) luminescent intensity subjected to β-gal (0, 1, 2, 4, 6, 8, 10 U mL<sup>-1</sup>) under 254 nm UV light.

almost identical. This indicates that Probe 1 has high selectivity in detecting β-gal.

The fluorescence-intensity changes of Probe 1 with various activities of β-gal (0, 0.01, 0.02, 0.04, 0.06, 0.08, 0.1, 0.2, 0.3, 0.4, 0.5, 0.6, 0.7, and 0.8 U mL<sup>-1</sup>) were recorded and are shown in Fig. 4a. The emission ratio ( $I_{444 \text{ nm}}/I_{374 \text{ nm}}$ ) exhibited two linear sections in response to β-gal activity: 0–0.1 U mL<sup>-1</sup> ( $R^2 = 0.9951$ , Fig. 4b) and 0.2–0.8 U mL<sup>-1</sup> ( $R^2 = 0.9968$ , Fig. 4c). The Probe 1 limit of detection (LOD) for β-gal activity was 0.0054 U mL<sup>-1</sup>, based on  $\text{LOD} = 3 \text{ SD/B}$ . This indicated that Probe 1 could be used to detect β-gal activity with a low LOD in water. In addition, the luminous intensity of Probe 1 gradually increased with increases in β-gal activity, as was observed by the naked eye under 254 nm UV irradiation (Fig. 4d). All results showed that Probe 1 could be used as a quantitative and qualitative tool to detect β-gal activity.

### 3.3 Recognition mechanism

After the addition of β-gal (1 U mL<sup>-1</sup>), a new peak appeared, which was previously proven to be compound 1 (Fig. S4, ESI†). Mass spectrometry provided further evidence that the β-galactosides were hydrolyzed (Fig. S5, ESI†), with the peak at  $m/z = 174.56.00$  corresponding to compound 1 (M – H); the peak at  $m/$

$z = 337.04$  was that of Probe 1 (M – H). These results show that Probe 1's mechanism for β-gal recognition is the β-gal enzymatic hydrolysis of β-galactosides.

### 3.4 Application

As β-gal activity is positively correlated with the maturity of fruit, the development of a simple and highly selective method for β-gal activity detection in fruit is crucial. Therefore, the ability of Probe 1 to detect β-gal activity in fruit must be demonstrated.

Pear, apple, grape, strawberry, and kiwi (20 μL) samples were tested using Probe 1. The β-gal activity of the kiwi (ripe) sample was  $0.0938 \pm 0.0027$  U mL<sup>-1</sup>, and those of the kiwi (unripe), pear, apple, grape, and strawberry samples were 0 U mL<sup>-1</sup> (Table 1). The ripeness of the kiwi fruit was mainly determined by the softness or hardness of the fruit (Fig. S6, ESI†).

To validate this method, the β-gal activity in these samples was tested using the β-galactosidase spectrophotometric method.<sup>40,41</sup> The β-gal activity of all samples was 0 U mL<sup>-1</sup>. No β-gal activity was detected in the kiwi (ripe) sample by the GB/T 33409-2016 method; this could be because the β-gal activity in kiwis (ripe) and the LOD of this method are of the same order of magnitude. Then, the addition of β-gal with different activities (0.02, 0.04, 0.2, and 0.4 U mL<sup>-1</sup>) to the samples showed that the



Table 1 Determination of  $\beta$ -gal activity in real fruit samples

Sample	$\beta$ -gal level found (U mL <sup>-1</sup> )	Added (U mL <sup>-1</sup> )	Found (U mL <sup>-1</sup> )	Recovery/%	RSD/% ( $n = 3$ )
Pear	0	0.02	0.022	108.00	0.11
		0.04	0.043	106.61	0.21
		0.2	0.221	101.32	1.69
		0.4	0.405	101.33	1.44
Apple	0	0.02	0.022	110.29	0.07
		0.04	0.044	108.94	0.33
		0.2	0.192	96.13	2.09
		0.4	0.387	96.71	6.31
Grape	0	0.02	0.022	108.80	0.26
		0.04	0.044	109.83	0.26
		0.2	0.217	108.32	1.40
		0.4	0.402	100.58	0.81
Strawberry	0	0.02	0.021	104.55	0.13
		0.04	0.041	101.86	0.19
		0.2	0.195	97.28	3.68
		0.4	0.376	94.07	1.33
Kiwi (unripe)	0	0.02	0.021	106.4	0.06
		0.04	0.041	103.39	0.08
		0.2	0.203	101.65	0.69
		0.4	0.403	100.63	1.89
Kiwi (ripe)	0.0938 $\pm$ 0.0027	—	—	—	—

recoveries ranged between 94.07–110.29% (Table 1). These results indicate that Probe 1 could accurately and quickly determine the  $\beta$ -gal activity in fruit.

## 4. Conclusions

In this study, a coumarin fluorescent probe (Probe 1) was developed for the ratiometric detection of  $\beta$ -gal activity. The mechanism of  $\beta$ -gal recognition by Probe 1 involves the  $\beta$ -gal enzymatic hydrolysis of  $\beta$ -galactosides. The quantitative range of  $\beta$ -gal activity detected was 0–0.1 U mL<sup>-1</sup> and 0.2–0.8 U mL<sup>-1</sup>, with an LOD of 0.0054 U mL<sup>-1</sup>. This method exhibited good linearity and specificity, had a short analytical time (30 min), required a small amount of sample (20  $\mu$ L), and had a low LOD. Additionally, the luminous intensity of Probe 1 gradually increased with increasing enzyme activity. This phenomenon could be observed by the naked eye under 254 nm UV irradiation. Furthermore, Probe 1 was a useful tool for the qualitative and quantitative determination of  $\beta$ -gal activity in fruit.

## Conflicts of interest

There are no conflicts of interest to declare.

## Acknowledgements

Thank you for the National Natural Science Foundation of China (31901770).

## References

- Q. Husain,  $\beta$  Galactosidases and their potential applications: a review, *Crit. Rev. Biotechnol.*, 2010, **30**, 41–62.
- Y. Tanaka, J. Kato, M. Kohara and M. S. Galinski, Antiviral effects of glycosylation and glucose trimming inhibitors on human parainfluenza virus type 3, *Antiviral Res.*, 2006, **72**, 1–9.
- D. C. Vieira, L. N. Lima, A. A. Mendes, W. S. Adriano, R. C. Giordano, R. L. Giordano and P. W. Tardioli, Hydrolysis of lactose in whole milk catalyzed by  $\beta$ -galactosidase from *Kluyveromyces fragilis* immobilized on chitosan-based matrix, *Biochem. Eng. J.*, 2013, **81**, 54–64.
- S. Rastegar, M. Rahemi, A. Baghizadeh and M. Gholami, Enzyme activity and biochemical changes of three date palm cultivars with different softening pattern during ripening, *Food Chem.*, 2012, **134**, 1279–1286.
- F. Tidona, A. Meucci, M. Povoio, V. Pelizzola, M. Zago, G. Contarini, D. Carminati and G. Giraffa, Applicability of *Lactococcus hircilactis* and *Lactococcus laudensis* as dairy cultures, *Int. J. Food Microbiol.*, 2018, **271**, 1–7.
- S. Mohebbi, M. Babalar, Z. Zamani and M. A. Askari, Influence of early season boron spraying and postharvest calcium dip treatment on cell-wall degrading enzymes and fruit firmness in 'Starking Delicious' apple during storage, *Sci. Hortic.*, 2020, **259**, 108822;
- M. Ishimaru, D. L. Smith, A. J. Mort and K. C. Gross, Enzymatic activity and substrate specificity of recombinant tomato  $\beta$ -galactosidases 4 and 5, *Planta*, 2009, **229**, 447–456.
- H. Lazan, S. Y. Ng, L. Y. Goh and Z. M. Ali, Papaya  $\beta$ -galactosidase/galactanase isoforms in differential cell wall hydrolysis and fruit softening during ripening, *Plant Physiol. Biochem.*, 2004, **42**, 847–853.
- A. Weber, D. A. Neuwald, D. Kitemann, F. R. Thewes, V. Both and A. Brackmann, Influence of respiratory quotient dynamic controlled atmosphere (DCA-RQ) and ethanol



- application on softening of Braeburn apples, *Food Chem.*, 2020, **303**, 125346.
- 10 A. Nakatsuka, T. Maruo, C. Ishibashi, Y. Ueda, N. Kobayashi, M. Yamagishi and H. Hiroyuki Itamura, Expression of genes encoding xyloglucan endotransglycosylase/hydrolase in 'Saijo' persimmon fruit during softening after deastringency treatment, *Postharvest Biol. Technol.*, 2011, **62**, 89–92;
  - 11 A. B. Bennett and J. M. Labavitch, Ethylene and ripening-regulated expression and function of fruit cell wall modifying proteins, *Plant Sci.*, 2008, **175**, 130–136.
  - 12 B. G. Defilippi, T. Ejsmentewicz, M. P. Covarrubias, O. Gudenschwager and R. Campos-Vargas, Changes in cell wall pectins and their relation to postharvest mesocarp softening of "Hass" avocados (*Persea americana* Mill.), *Plant Physiol. Biochem.*, 2018, **128**, 142–151.
  - 13 A. Tateishi, H. Inoue, H. Shiba and S. Yamaki, Molecular cloning of  $\beta$ -galactosidase from Japanese pear (*Pyrus pyrifolia*) and its gene expression with fruit ripening, *Plant Cell Physiol.*, 2001, **42**, 492–498.
  - 14 S. Guo, J. Song, B. Zhang, H. Jiang, R. Ma and M. Yu, Genome-wide identification and expression analysis of beta-galactosidase family members during fruit softening of peach [*Prunus persica* (L.) Batsch], *Postharvest Biol. Technol.*, 2018, **136**, 111–123.
  - 15 X. Zheng, G. Jing, Y. Liu, T. Jiang, Y. Jiang and J. Li, Expression of expansin gene, MiExpA1, and activity of galactosidase and polygalacturonase in mango fruit as affected by oxalic acid during storage at room temperature, *Food Chem.*, 2012, **132**, 849–854.
  - 16 S. Boelz, G. Neu-Yilik, N. H. Gehring, M. W. Hentze and A. E. Kulozik, A chemiluminescence-based reporter system to monitor nonsense-mediated mRNA decay, *Biochem. Biophys. Res. Commun.*, 2006, **349**, 186–191.
  - 17 D. Farquhar, B. Pan, M. Sakurai, A. Ghosh, C. A. Mullen and A. J. Nelson, Suicide gene therapy using *E. coli*  $\beta$ -galactosidase, *Canc. Chemother. Pharmacol.*, 2002, **50**, 65–70.
  - 18 J. Chen, Z. Jiang, J. D. Ackerman, M. Yazdani, S. Hou, S. R. Nugen and V. M. Rotello, Electrochemical nanoparticle–enzyme sensors for screening bacterial contamination in drinking water, *Analyst*, 2015, **140**, 4991–4996.
  - 19 A. Y. Louie, M. M. Hüber, E. T. Ahrens, U. Rothbacher, R. Moats, R. E. Jacobs, S. E. Fraser and T. J. Meade, In vivo visualization of gene expression using magnetic resonance imaging, *Nat. Biotechnol.*, 2000, **18**, 321–325.
  - 20 G. Andreotti, A. Trincon and A. Giordano, Convenient synthesis of  $\beta$ -galactosyl nucleosides using the marine  $\beta$ -galactosidase from *Aplysia fasciata*, *J. Mol. Catal. B: Enzym.*, 2007, **47**, 28–32.
  - 21 S. J. Kim, D. J. Doudet, A. R. Studenov, C. Nian, T. J. Ruth, S. S. Gambhir and C. H. S. McIntosh, Quantitative micro positron emission tomography (PET) imaging for the *in vivo* determination of pancreatic islet graft survival, *Nat. Med.*, 2006, **12**, 1423–1428.
  - 22 T. Naqvi, A. Lim, R. Rouhani, R. Singh and R. M. Eglén, Galactosidase enzyme fragment complementation as a high-throughput screening protease technology, *J. Biomol. Screen.*, 2004, **9**, 398–408.
  - 23 T. Tschirhart, X. Y. Zhou, H. Ueda, C. Y. Tsao, E. Kim, G. F. Payne and W. E. Bentley, Electrochemical measurement of the  $\beta$ -galactosidase reporter from live cells: a comparison to the Miller assay, *ACS Synth. Biol.*, 2016, **5**, 28–35.
  - 24 X. Kong, M. Li, B. Dong, Y. Yin, W. Song and W. Lin, An ultrasensitivity fluorescent probe based on the ICT-FRET dual mechanisms for imaging  $\beta$ -galactosidase *in vitro* and *ex vivo*, *Anal. Chem.*, 2019, **91**, 15591–15598.
  - 25 J. Liu, H. Bao, C. Liu, F. Wu and F. Gao, "Turn-On" Fluorescence Determination of  $\beta$ -Glucosidase Activity Using Fluorescent Polymer Nanoparticles Formed from Polyethylenimine Cross-Linked with Hydroquinone, *ACS Appl. Polym. Mater.*, 2019, **1**, 3057–3063.
  - 26 J. Zhang, P. Cheng and K. Pu, Recent Advances of Molecular Optical Probes in Imaging of  $\beta$ -Galactosidase, *Bioconjugate Chem.*, 2019, **30**, 2089–2101.
  - 27 R. Gui, H. Jin, X. Bu, Y. Fu, Z. Wang and Q. Liu, Recent advances in dual-emission ratiometric fluorescence probes for chemo/biosensing and bioimaging of biomarkers, *Coord. Chem. Rev.*, 2019, **383**, 82–103.
  - 28 X. Bu, Y. Fu, X. Jiang, H. Jin and R. Gui, Self-assembly of dna-templated copper nanoclusters and carbon dots for ratiometric fluorometric and visual determination of arginine and acetaminophen with a logic-gate operation, *Microchim. Acta*, 2020, **187**, 154.
  - 29 X. Jiang, H. Jin, Y. Sun, Z. Sun and R. Gui, Assembly of black phosphorus quantum dots-doped mof and silver nanoclusters as a versatile enzyme-catalyzed biosensor for solution, flexible substrate and latent fingerprint visual detection of baicalin, *Biosens. Bioelectron.*, 2020, **152**, 112012.
  - 30 H. W. Liu, L. Chen, C. Xu, Z. Li, H. Zhang, X. B. Zhang and W. Tan, Recent progresses in small-molecule enzymatic fluorescent probes for cancer imaging, *Chem. Soc. Rev.*, 2018, **47**, 7140–7180.
  - 31 N. Hananya, A. Eldar Boock, C. R. Bauer, R. Satchi-Fainaro and D. Shabat, Remarkable Enhancement of Chemiluminescent Signal by Dioxetane–Fluorophore Conjugates: Turn-ON Chemiluminescence Probes with Color Modulation for Sensing and Imaging, *J. Am. Chem. Soc.*, 2016, **138**, 13438–13446.
  - 32 T. S. Wehrman, G. von Degenfeld, P. O. Krutzik, G. P. Nolan and H. M. Blau, Luminescent Imaging of  $\beta$ -Galactosidase Activity in Living Subjects using Sequential Reporter-Enzyme Luminescence. *Nat. Methods*, 2006, **3**, 295–301.
  - 33 H. W. Lee, C. H. Heo, D. Sen, H. O. Byun, I. H. Kwak, G. Yoon and H. M. Kim, Ratiometric Two-Photon Fluorescent Probe for Quantitative Detection of  $\beta$ -Galactosidase Activity in Senescent Cells, *Anal. Chem.*, 2014, **86**, 10001–10005.
  - 34 B. Lozano-Torres, I. Galiana, M. Rovira, E. Garrido, S. Chaib, A. Bernardos, D. Muñoz-Espín, M. Serrano, R. Martínez-Mañez and F. Sancenón, An OFF–ON Two-Photon Fluorescent Probe for Tracking Cell Senescence in Vivo, *J. Am. Chem. Soc.*, 2017, **139**, 8808–8811.



- 35 K. Gu, Y. Xu, H. Li, Z. Guo, S. Zhu, S. Zhu, P. Shi, T. D. James, H. Tian and W. H. Zhu, Real-Time Tracking and *In Vivo* Visualization of  $\beta$ -Galactosidase Activity in Colorectal Tumor with a Ratiometric Near-Infrared Fluorescent Probe, *J. Am. Chem. Soc.*, 2016, **138**, 5334–5340.
- 36 E. J. Kim, R. Kumar, A. Sharma, B. Yoon, H. M. Kim, H. Lee, K. S. Hong and J. S. Kim, In Vivo Imaging of  $\beta$ -Galactosidase Stimulated Activity in Hepatocellular Carcinoma using Ligand-Targeted Fluorescent Probe, *Biomaterials*, 2017, **122**, 83–90.
- 37 C. H. Tung, Q. Zeng, K. Shah, D. E. Kim, D. Schellingerhout and R. Weissleder, In Vivo Imaging of  $\beta$ -Galactosidase Activity Using Far Red Fluorescent Switch, *Cancer Res.*, 2004, **64**, 1579–1583.
- 38 D. Oushiki, H. Kojima, Y. Takahashi, T. Komatsu, T. Terai, K. Hanaoka, M. Nishikawa, Y. Takakura and T. Nagano, Near-Infrared Fluorescence Probes for Enzymes Based on Binding Affinity Modulation of Squarylium Dye Scaffold, *Anal. Chem.*, 2012, **84**, 4404–4410.
- 39 J. Zhang, C. Li, C. Dutta, M. Fang, S. Zhang, A. Tiwari, F. Luo and H. Liu, A novel near-infrared fluorescent probe for sensitive detection of  $\beta$ -galactosidase in living cells, *Anal. Chim. Acta*, 2017, **968**, 97–104.
- 40 Y. Li, N. Duan, X. Wu, S. Yang, H. Tian and B. Sun, Novel fluorescent probe for the ratiometric detection of  $\beta$ -galactosidase and its application in fruit, *Food Chem.*, 2020, **328**, 127112.
- 41 N. Duan, H. Wang, Y. Li, S. Yang, H. Tian and B. Sun, The research progress of organic fluorescent probe applied in food and drinking water detection, *Coord. Chem. Rev.*, 2021, **427**, 213557.

